Additional File 3: 3D inversion details, data and model responses

A) 3D geoelectrical model using a NS-EW oriented grid

We created a homogeneous model of 100 ohm·m with a mesh of 76 (4.2 km NS) x 100 (4.8 km EW) x 55 (12 km z), including the topography (Figure S3-1a). In the central part the width of the cells was 20 m by 20 m and increased by a factor of 1.2 towards the edges. The thickness of the cells were of 20 m at the top 320 m (coinciding with the topography), increased to 30 m down to 770 m and to 50 m down to 1520 m. From this depth the thicknesses increased progressively from 100 m to 5000 m.

For the inversion considering the ZI transfer functions, we used data from all the sites except for site 4 and 13, which were on the other side of the highway, hence very noisy, and also too far from the target of the fault zone. Thus, we had a dataset with 13 sites, 7 of which (sites 1, 3, 5, 7, 9, 11 and 12) had local electric and magnetic signals recorded, so the transfer function used was Z. The remaining sites only had the electric records and used the magnetic from a remote site and hence the transfer functions were ZI: site

2(E:2;B:1); site 6(E:6;B:5); site 8(E:8;B:7); site 10(E:10;B:7); site 14(E:14;B11) and site 15(E:15;B:11). We chose a period range between 10^{-3} s and 10^{2} s and at each period we set the same error for the diagonal and off-diagonal components, which was a 5% error of the off-diagonal components. Additionally, we made a visual inspection of all the components at all sites and removed data from some of the frequencies.

We used a smoothing factor of 0.4, a trade-off parameter of 1 and an initial search step of 20. The initial rms was 12.13 and it converged to 6.23 after 95 iterations, when the inversion reached a local minimum. The overall rms and the rms for each component for the individual sites are plotted in Figure S3-1a. In general, the poorest fits are obtained for the diagonal components. Figure S3-1b shows a cross section that goes approximately along the locations of the sites and 3 horizontal slices of the resulting model at different depths. At shallow depths (down to 200 m.a.s.l.) the model is characterised by high resistivities (500 – 1000 ohm·m); with some conductive areas within it in the southeastern part. The main conductor is located below sites 1, 2 and 12 (with resistivities down to less than 1 ohm·m and reaches a maximum depth of 250 m.a.s.l. A second

conductor appears at the SE end of the profile, below site 14, and has more moderate resistivity values (down to 5 ohm·m) and reaches higher depths (200 m.a.s.l.). Between these two conductors, smaller conductors are placed at very shallow levels. Below it, the model is very homogeneous, with resistivities ranging between 20 and 100 ohm·m. Below 400 m depth (- 400 m.a.s.l.), the model preserves the 100 ohm·m of the initial model. In the shallow part, the upper resistor UR and the U-C alternation from the 2D model (Figure 9) can be identified. The large central conductor can be identified as C2, but it is clearly not as deep as in the 2D model.

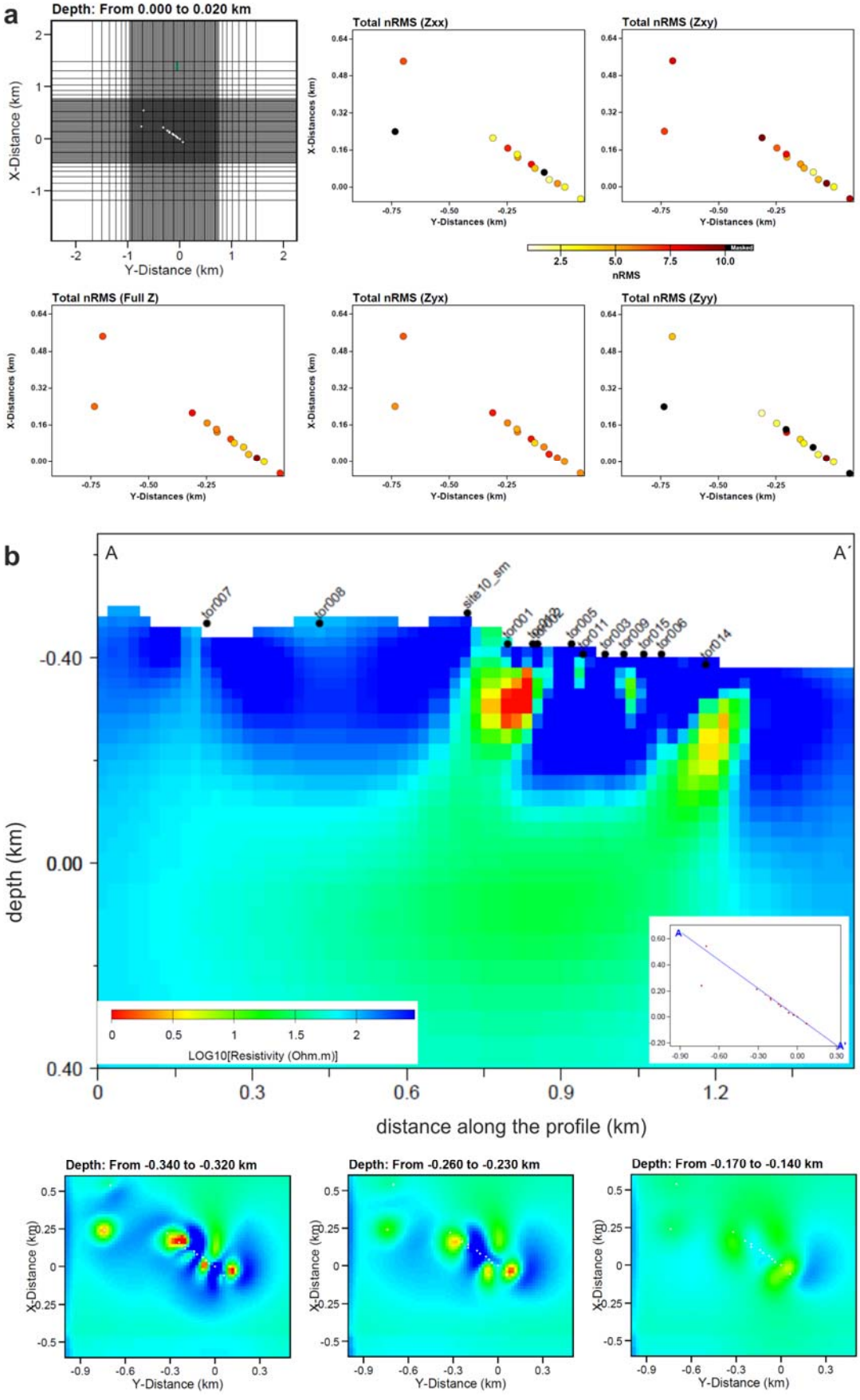
a
Depth: From 0.000 to 0.020 km
X-Distance (km)
Y-Distance (km)
Total nRMS (Zxx)
Total nRMS (Zxy)
Total nRMS (Full Z)
Total nRMS (Zyx)
Total nRMS (Zyy)
X-Distances (km)
Y-Distances (km)
2.5
5.0
7.5
10.0
nRMS
b
A
A´
tor007
tor008
site10_sm
tor001
tor005
tor011
tor003
tor009
tor015
tor006
tor014
depth (km)
-0.40
0.00
0.40
0
0.3
0.6
0.9
1.2
distance along the profile (km)
0
0.5
1
1.5
2
LOG10[Resistivity (Ohm.m)]
Depth: From -0.340 to -0.320 km
Depth: From -0.260 to -0.230 km
Depth: From -0.170 to -0.140 km
X-Distance (km)
Y-Distance (km)

Figure S3-1 a) Top left: Plain view of the mesh used with the location of sites. Top right: map of the overall rms at each site. Central to bottom: rms maps of the 4 components inverted. b) cross section of the model obtained from the inversion of ZI along AA', some of the sites have been projected for reference. c) plan view of the central part of the model obtained at the shallowest depths.

The inversion of qZ was performed using the same initial model and parameters. The rms decreased from 12.24 to 6.03 after 110 iterations. The resulting model (Figure S3-2) shows similar shallow features and the main conductor (C1) can be identified, which has higher resistivities than in the ZI model, reaches higher depths and has a more vertical trend.

Even though the quality of the data is far from ideal given the high level of noise, we can extract some conclusions from the 3D inversion results of ZI and qZ. We can observe that, on the NW side of the model, below sites 8 and 10, which use the magnetic from site 7, the model seems to be insensitive to the use of qZ instead of ZI, even though site 7 is

located over a resistive zone. In the central part, sites 2 is relatively close to the remote site 1, but the location, resistivity and shape of the central conductor is significantly different from both models. On the SE end, the differences are also evident and can be attributed to the longest distance between the local and the remote sites.

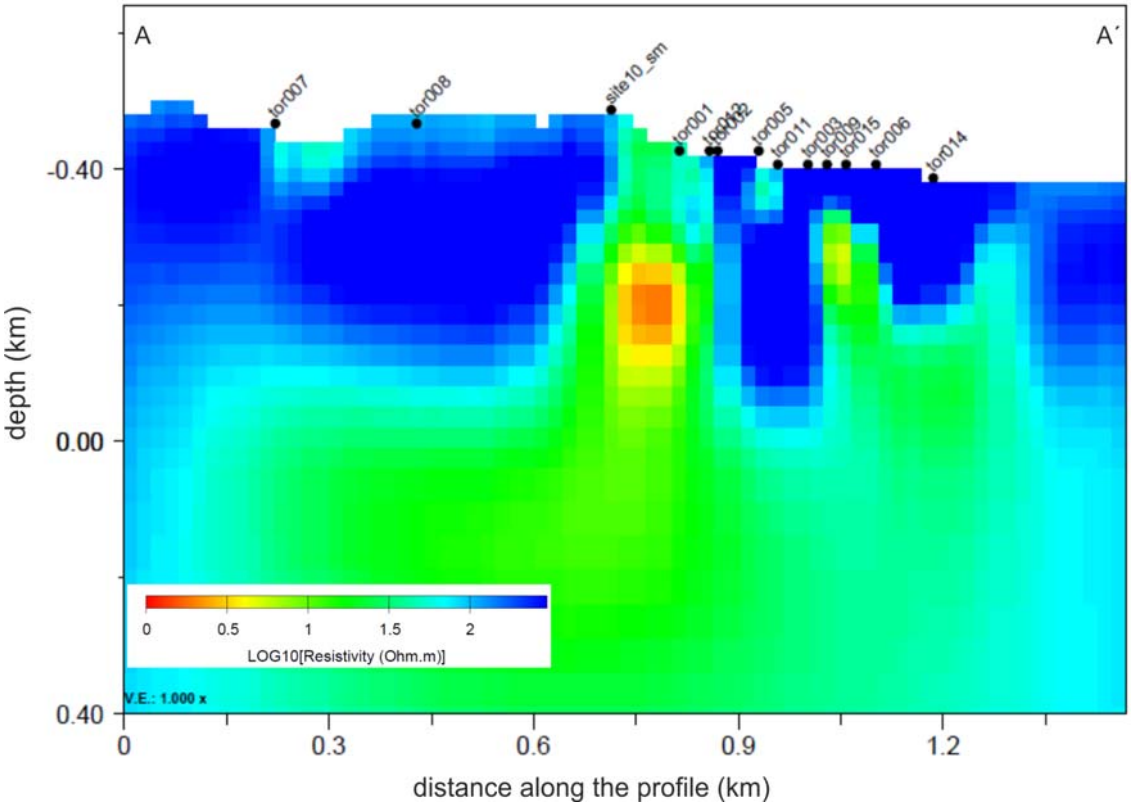

Figure S3-2: Cross section of the model obtained from the inversion of qZ along AA' (same orientation as in figure S3-1), some of the sites have been projected for reference.

B) Mesh and inversion parameters for the 3D geoelectrical model rotated 40ºNE

Mesh sizes: 54 (18 km NS) x 64 (19 km EW) x 63 (15 km z), including the topography.

Central part: the width of the cells was 23 m by 23 m and increased by a factor of 1.5 towards the edges. The thickness of the cells were of 50 m (air layers) or 25 m down to -500 m.a.s.l., and increased a factor of 1.4 down to 15 km.

Inverted data: Off-diagonal components, after manually deactivating frequencies with peaks. Sites 7, 10, 1, 12, 5, 1, 3, 9, 15 and 14. Periods 10^{-3} s and 10^{2} s. 10 % error .

Inversion parameters and results:

Initial model: 2D model extended to all the model slices parallel to the data.

Smoothing factor: 0.2, trade-off parameter: 1; initial search step of 20.

Initial rms = 14.49; final rms (48 iterations) = 3.06.

C) Data and model responses for the 3D geoelectrical model rotated 40ºNE:

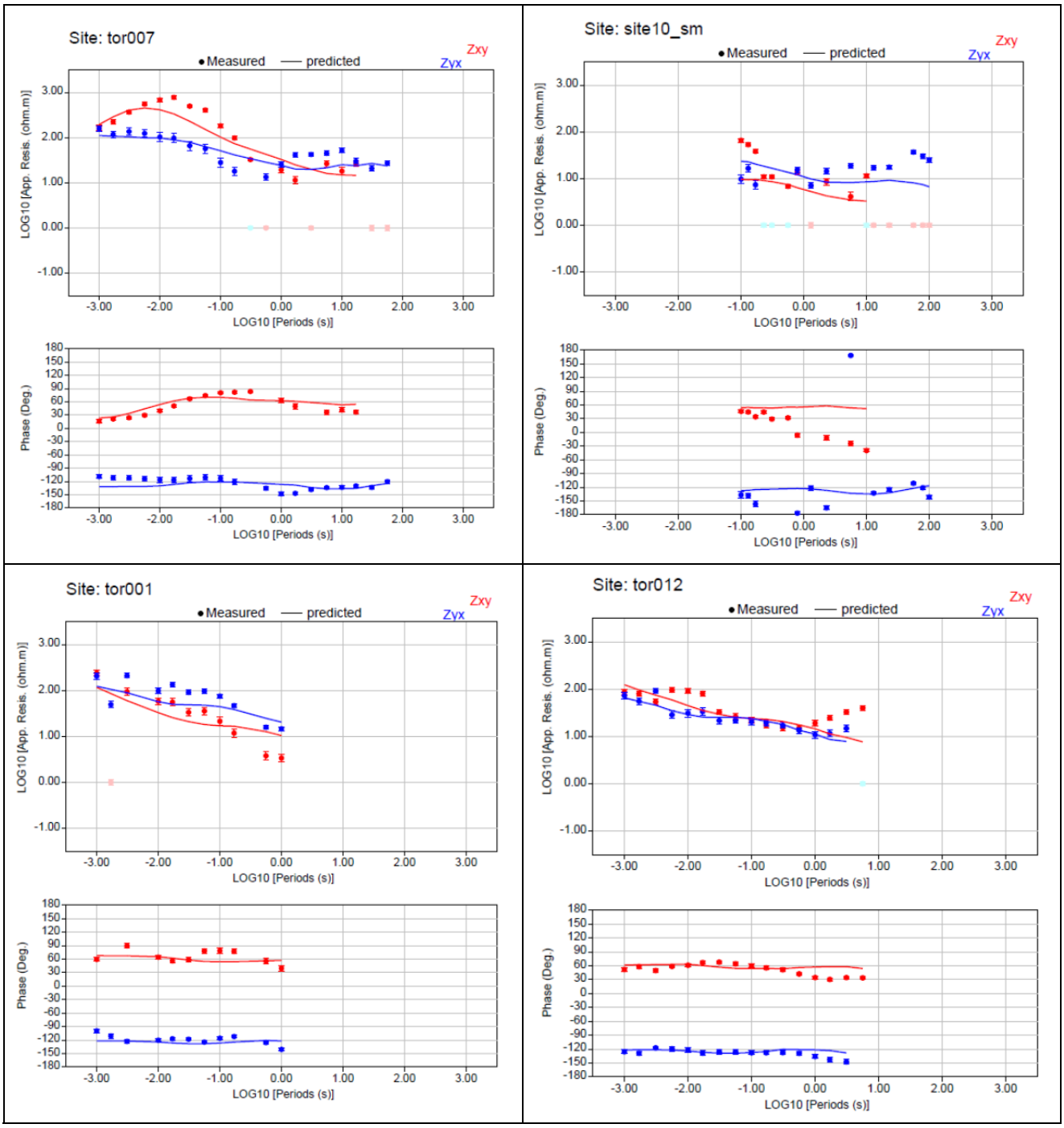

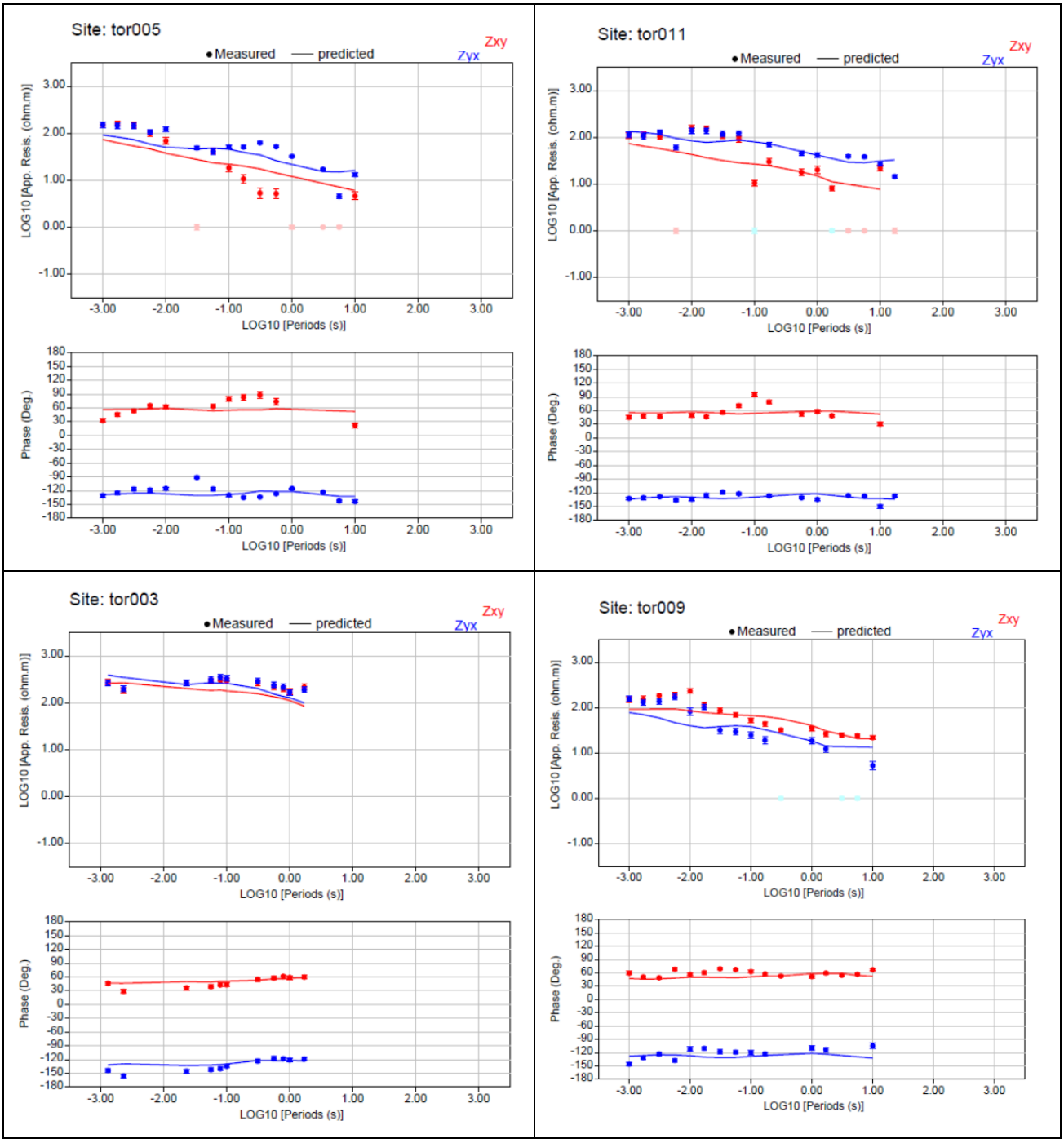
Site: tor005
Measured
predicted
Zxy
Zyx
LOG10 [App. Resis. (ohm.m)]
LOG10 [Periods (s)]
Phase (Deg.)
Site: tor011
Measured
predicted
Zxy
Zyx
LOG10 [App. Resis. (ohm.m)]
LOG10 [Periods (s)]
Phase (Deg.)
Site: tor003
Measured
predicted
Zxy
Zyx
LOG10 [App. Resis. (ohm.m)]
LOG10 [Periods (s)]
Phase (Deg.)
Site: tor009
Measured
predicted
Zxy
Zyx
LOG10 [App. Resis. (ohm.m)]
LOG10 [Periods (s)]
Phase (Deg.)

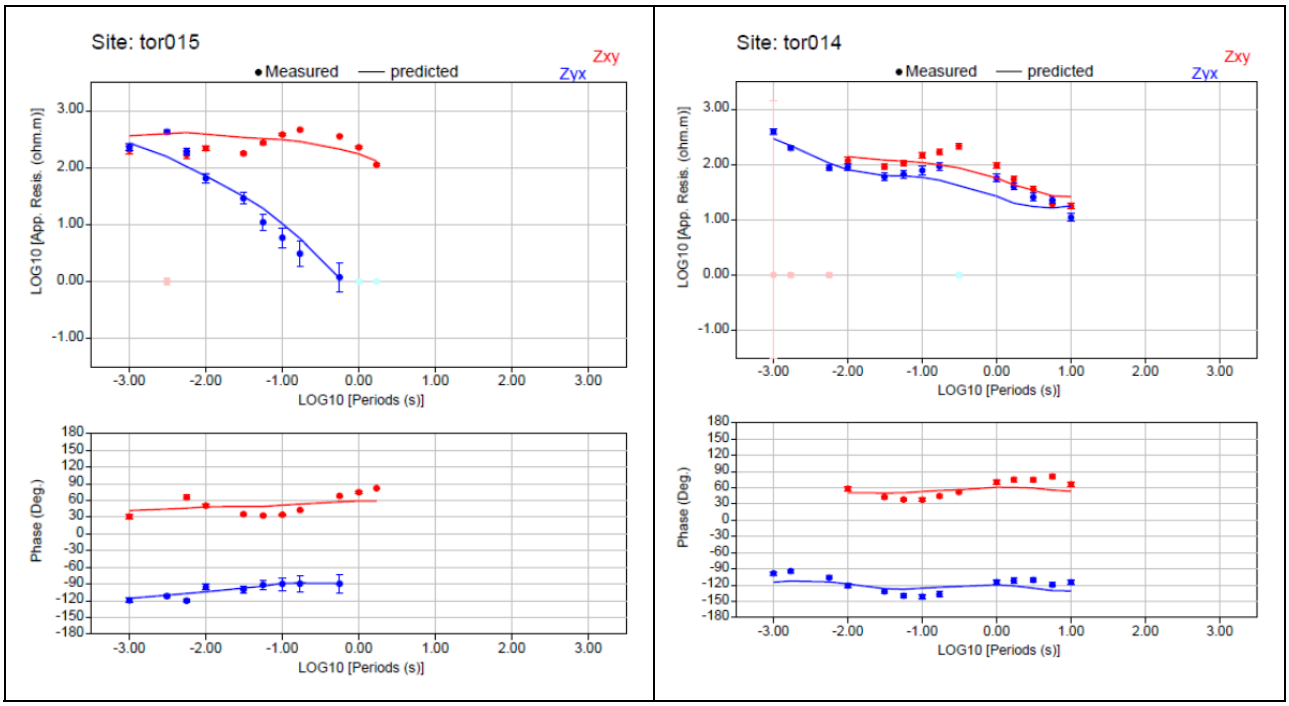

Figure S3-3: Data (dots) and model responses (lines) for the 3D geoelectrical model rotated 40ºNE.